Highly efficient degradation of PFAS and other surfactants in water with atmospheric RAdial Plasma (RAP) discharge

Mubbshir Saleem*, Giulia Tomei, Matteo Beria, Ester Marotta*, Cristina Paradisi

Department of Chemical Sciences, University of Padova, Via Marzolo 1, 35131 Padova, Italy

***Corresponding authors**

Ester Marotta,

Department of Chemical Sciences, University of Padova, Via Marzolo 1, 35131 Padova, Italy.

Email: ester.marotta@unipd.it

Mubbshir Saleem,

Department of Chemical Sciences, University of Padova, Via Marzolo 1, 35131 Padova, Italy.

Email: mubasher_sky@hotmail.com; mubbshir.saleem@unipd.it

Abstract

Atmospheric plasma offers a viable approach to new water remediation technologies, best suited for the degradation of persistent organic pollutants such as PFAS, per- and polyfluoroalkyl substances. This paper reports on the remarkable performance of a novel RAdial Plasma (RAP) discharge reactor in treating water contaminated with PFAS surfactants, notably the ubiquitous perfluorooctanoic acid (PFOA) and perfluorooctanesulfonic acid (PFOS). RAP proved to be versatile and robust, performing very well over a wide range of pollutants concentrations. Thus, PFOA degradation was most satisfactory with regard to all critical indicators, kinetics (≥ 99% PFOA conversion in less than 2.5 min and 30 min in solutions with initial concentrations of 41 μg/L and 41 mg/L, respectively), byproducts, and energy efficiency (G_{50} greater than 2000 mg/kWh for 41 μg/L – 4.1 mg/L PFOA initial concentrations). Likewise for PFOS as well as for Triton X-100, a common fluorine-free non-ionic surfactant tested to explore the scope of applicability of RAP to the degradation of surfactants in general. The results obtained with RAP compare most favourably with those reported for state-of-art plasma systems in similar experiments. RAP's excellent performance is attributed to the dense network of radial discharges it generates, randomly spread over the entire exposed surface of the liquid thus establishing an extended highly reactive plasma-liquid interface with both strongly reducing and oxidizing species. Mechanistic insight is offered based on the observed degradation products and on available literature data on the surfactants properties and on their plasma induced degradation investigated in previous studies.

Keywords:

Atmospheric plasma; PFAS degradation; water treatment; plasma treatment energy efficiency; PFOA; PFOS

1. Introduction

Contamination of waters and soils by manmade, highly persistent per- and polyfluoroalkyl substances (PFAS) has become a major global ecological threat (Podder et al., 2021). Specifically, there is growing evidence for serious health hazards to humans exposed to PFAS contained in drink and foodstuff (Podder et al., 2021). Since conventional water and wastewater treatment systems are ineffective, PFAS are usually removed by sorption (Kah et al., 2021). Disposal of PFAS loaded spent sorbents, however, raises so many issues, in terms of risks and additional costs, that "suitable destruction methods need to be developed" (Kah et al., 2021). This is indeed a great challenge, since PFAS are not attacked by OH radicals and advanced oxidation processes, which rely on the production and action solely of OH radicals, have no or only limited efficacy in their removal. Advanced oxidation/reduction processes offer better promise (Trojanowicz et al., 2018), with atmospheric pressure plasmas being reported as the most energy efficient in achieving high degrees of PFAS mineralization (Nzeribe et al., 2019). Atmospheric plasmas are non-equilibrium systems which can be readily generated by various types of electric discharges injecting high energy electrons in a gas at atmospheric pressure and temperature. Gas/electron interactions produce highly reactive short-lived species including ions, radicals, and various excited species. When formed in contact with or in proximity to the water to be treated, the plasma reactive species diffuse into and/or react with water leading to a mix of powerful oxidants and reductants, including notably hydrated electrons and OH radicals, capable of initiating the chemical degradation of any organic contaminant present, including the most recalcitrant PFAS (Bulusu et al., 2020; Groele et al., 2021; Hayashi et al., 2015; Lewis et al., 2020; Mahyar et al., 2019; Rabinovich et al., 2022; Saleem et al., 2020a; Stratton et al., 2017; Takeuchi et al., 2020, 2014; Zhang et al., 2021). Atmospheric plasma is perceived as a green approach to water treatment since it only needs electricity and no added chemicals or catalysts, thus avoiding the costs associated with their use and consumption and with disposal of their byproducts. Moreover, atmospheric plasmas do not require heat or cooling, pressure or vacuum, and are easily and quickly switched on and off. Several configurations and

types of discharges have been tested for PFAS atmospheric plasma induced degradation. The most promising ones, achieving PFAS degradations of ⩾90% with high energy efficiencies employ plasma generated within gas bubbles inside the liquid (Hayashi et al., 2015; Obo et al., 2015; Saleem et al., 2020a; Takeuchi et al., 2014), streamer or leader discharges in contact with the liquid surface (Saleem et al., 2020a; Stratton et al., 2017; Zhang et al., 2021), submerged reverse vortex gliding arc plasmatron (Lewis et al., 2020) and plasma-jet inside the liquid (Groele et al., 2021). Most investigations deal with perfluorooctanoic acid (PFOA) and perfluorooctanesulfonic acid (PFOS), two of the most important and ubiquitous representatives of the PFAS family, which in water are fully ionized and display strong surface activity. The results obtained with these surfactants strongly suggest that initial attack on PFAS occurs at the plasma-liquid interface and that electrons, free and hydrated, are involved in this crucial first step (Saleem et al., 2020a; Stratton et al., 2017; Takeuchi et al., 2014; Zhang et al., 2021). Despite the significant progress recently made in the characterization of these reactions, fundamental research is still needed to fully characterize the complex physical chemical processes occurring in the heterogeneous system composed of gas/plasma/liquid and at the corresponding interfaces. At the same time, reports are beginning to appear which describe preliminary promising efforts at scaling up and implementation of this approach into a new technology (Rabinovich et al., 2022; Thagard and Locke, 2022). Performance optimization is thus the issue on which much current research is focused, major indicators to be considered being the reactor design and its energy efficiency, the process kinetics and the types, properties and amounts of degradation by-products.

This paper reports the excellent results we obtained in the degradation of the two common PFAS perfluorooctanoic acid (PFOA) and perfluorooctanesulfonic acid (PFOS) in tap water using a novel proprietary RAdial Plasma discharge (RAP) reactor (Saleem et al., 2020b). RAP's performance was assessed based on kinetics and energy efficiency, and compared with that of relevant state-of-art plasma reactors in analogous experiments. To test the scope of applicability of RAP to the treatment of surface active pollutants in general, a few experiments were also performed with Triton X-100, a

very common non-ionic, non-fluorinated surfactant. The results obtained show the robustness of the novel RAP discharge in degrading surfactants with excellent energy efficiency as compared with the state of the art.

2. Materials and methods

2.1. Experimental set-up

A RAdial Plasma (RAP) discharge reactor was used consisting of a 128 mm high and 43 mm diameter cylindrical Pyrex vessel fitted with an airtight Plexiglas cover and with a fritted glass diffuser fixed 17.5 mm above the cylinder base (Figure 1). The cover has a hole for the gas out flow and a concentric hole for supporting the pointed edge high voltage tungsten electrode (2.5 mm diameter) placed 6 mm above the liquid surface. The counter electrode is a stainless-steel ring (39 mm diameter) held partially submerged in the liquid. Argon, used as plasma feed gas, was bubbled into the liquid at a flowrate of 100 mL/min through the fritted glass septum at the bottom of the reactor.

Plasma was ignited with a Spellman PTV30*350 (30 kV, 12 mA) high voltage power supply with negative polarity and protected by a 2.5 MΩ high voltage resistor. Due to the specific configuration and reciprocal arrangement of the opposing electrodes, numerous random radial discharges contacting the liquid surface and sweeping between the opposing electrodes are generated. These discharges cover the entire area encircled by the grounded electrode and hence provide a dense and most effective plasma-liquid interface. The input power was maintained at 4 W by regulating the pulse frequency between 60-80 Hz by charging a high voltage capacitor (2.1 nF), connected in parallel to the RAP reactor.

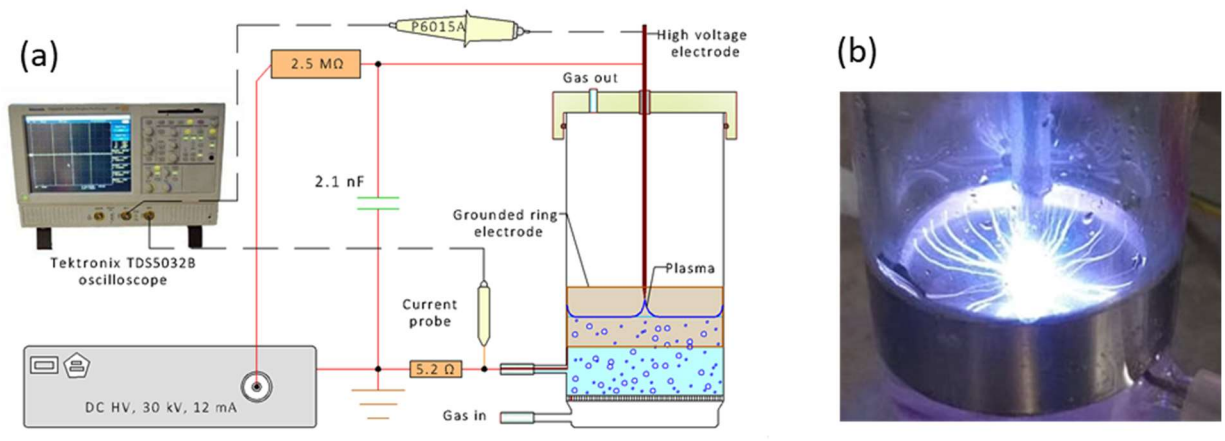

Figure 1. a) Schematic representation of the experimental setup. b) Photograph of the discharge.

2.2. Determination of the dissipated power for the RAP reactor

The voltage was measured using a high voltage probe, Tektronix P6015A, connected to a Tektronix TDS5032B oscilloscope (350 MHz, 5 GS/s) while the current was measured by determining the voltage drop across a non-inductive resistor (5.2 Ω) mounted between the ring electrode and the grounding point, using an ordinary voltage probe as shown in Figure 1. An example of voltage and current waveforms is presented in Fig. 2.

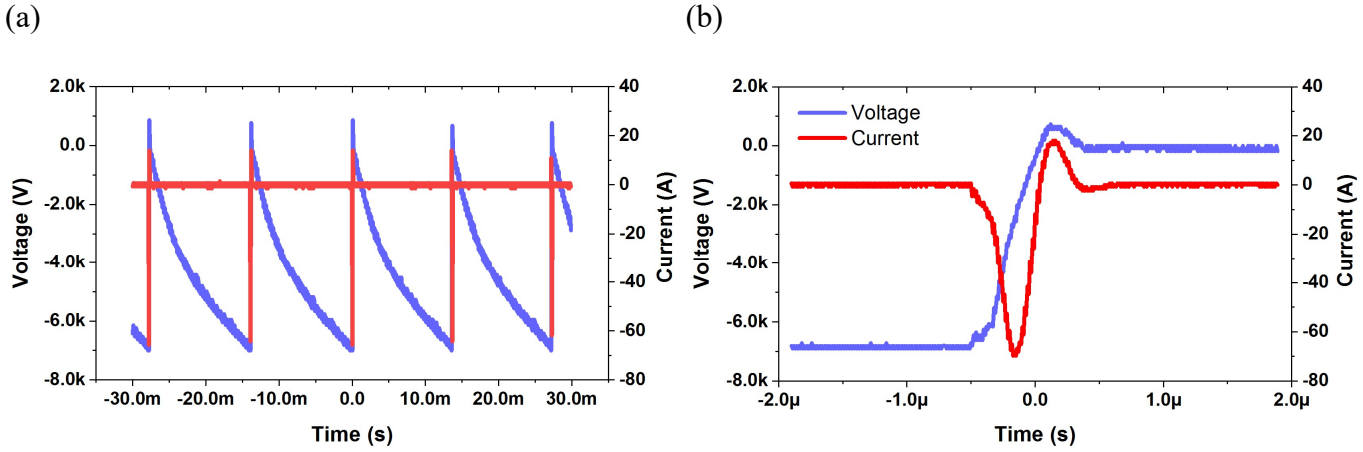

Figure 2 Typical voltage and current waveforms for RAP discharge at two different time scales (a) multiple waveforms and (b) single waveform.

125 The power dissipated in the RAP reactor corresponded to the product of energy deposited in the
126 capacitor before the breakdown and the discharge frequency. The deposited charge of the capacitor
127 determined the energy of the single pulse (Ep) (Fig. 2b) in the RAP reactor and was calculated
128 using Eq. (1).

$$E = \frac{1}{2} C V^2 \quad (1)$$

129 where C is the capacitance and V is the applied voltage. The calculated energy for a single pulse
130 (Fig. 2a) using Eq.1 was 0.0514 J. The energy of a single pulse (Fig. 2b) was also measured by
131 integrating the product of voltage (u) and current (i) waveform over time using Eq. 2 giving a value
132 of 0.0512 J. The measurements confirmed the validity of the pulse energy determination using Eq.1,
133 and the accuracy of the used method was within 1%.

$$E_{pulse} = \int_0^{\tau} u(t) \cdot i(t) \cdot dt \quad (2)$$

134 Average power for the RAP reactor was then calculated as the integral of the measured powers
135 during the treatment divided by the time of treatment.
136
137 **2.3. Chemicals**
138 Perfluorooctanoic acid (PFOA, reagent grade purity ⩾ 96%), Perfluoroheptanoic acid (PFHpA,
139 reagent grade purity 99 %), Perfluorohexanoic acid (PFHxA, reagent grade purity ⩾ 98 %),
140 Perfluoropentanoic acid (PFPA, reagent grade purity ⩾ 98 %), Perfluorobutanoic acid (PFBA,
141 reagent grade purity ⩾ 98 %), Triton X-100, perfluorooctanesulfonic acid potassium salt (PFOS,
142 reagent grade purity ⩾ 98 %) and methanol (HPLC PLUS grade 99.9%) were purchased from
143 Sigma-Aldrich. Ammonium acetate (reagent grade purity ⩾ 98%) was obtained from Fluka. Argon
144 was purchased from Air Liquide with specified impurities of H_2O (<0.5 ppm), of H_2 (<0.1 ppm), O_2
145 (<0.5 ppm), of CO_2 (<0.5 ppm), of CO (<0.1 ppm) and THC (<0.1 ppm). Tap water, drawn from the

lab drinking water faucet, had physical properties and chemical composition as described in a previous publication (Marotta et al., 2012).

2.4. Procedures and determination of the process kinetic coefficient and energy efficiency

Degradation experiments were performed with prepared PFOA and PFOS solutions in tap water at initial concentrations of $1 \cdot 10^{-4}$ M, $1 \cdot 10^{-5}$ M and $1 \cdot 10^{-7}$ M. The reported concentrations of PFAS in environmental matrices are typically lower i.e. in the ppb-ppt range (Podder et al., 2021), and therefore, the experiments conducted using an initial concentration of $1 \cdot 10^{-7}$ M on PFAS sample was more representative of the actual scenario. However, in order to more clearly investigate the generation of shorter-chain by-products from PFAS degradation, experiments were also performed at initial PFAS concentrations of $1 \cdot 10^{-4}$ M and $1 \cdot 10^{-5}$ M. Additionally, experiments were also conducted on prepared solution of Triton X-100 ($1 \cdot 10^{-5}$ M and $1 \cdot 10^{-4}$ M) in order to demonstrate the ability of the novel RAP discharge in degrading fluorinated and non-fluorinated surfactants with high energy efficiencies. For each concentration the reaction progress and products were monitored by performing batch experiments, with 30 mL aliquots of the prepared solution treated in the RAP reactor for selected times. Each PFAS treated sample was then analysed by LC-ESI/MS to determine the residual PFOA or PFOS concentration and to detect and identify its products. Analyses were carried out with an HPLC Agilent 1200 series chromatograph coupled with a Thermo Scientific LTQ XL mass spectrometer equipped with an electrospray source and a linear ion trap analyser. The chromatographic separation was performed using an InfinityLab Poroshell 120 EC-C18 2.1 X 100 mm 2.7 μm column (Agilent Technologies). The eluents used consist in ammonium acetate 5 mM in Milli-Q water (A) and methanol (B). The gradient for eluent B was as follows: from 30% to 100% in 13 minutes, isocratic at 100% for 8 minutes. The flow rate was set at 0.3 mL/min and the injection volume was 10 μL. Samples ionization was performed in negative mode (ESI-), with a spray of 2.5 kV and a source temperature of 300 °C. Optimized values for

auxiliary gas flows were the following: Sheath gas = 35 a.u., Auxiliary gas = 10 a.u., Sweep gas = 0 a.u.. The quantification of PFOA $[M-H]^-$ (m/z 413), PFOS $[M-H]^-$ (m/z 499), PFHeA $[M-H]^-$ (m/z 363), PFHxA $[M-H]^-$ (m/z 313), PFPA $[M-H]^-$ (m/z 263) and PFBA $[M-H]^-$ (m/z 213) was based on external calibration curves, using perfluorononanoic acid (PFNA) $[M-H]^-$ (m/z 463) as internal standard.

The residual concentration of Triton X-100 in the treated samples was instead measured by HPLC-UV analysis using an Agilent 1260 Infinity series II instrument equipped with a variable wavelength detector and a Phenomenex Kinetex® 4.6 x 150 mm 5 μm C18 100 Å column. The eluents were H_2O (solvent A) and methanol (solvent B) with the following gradient for B: t = 0 min 40%, t = 5 min 70%, t = 12 min 100%, t = 13 min 100%. The flow rate was set at 1 mL/min and the injection volume was 20 µL. Elution was followed at 225 nm.

The residual concentrations of the considered contaminant were interpolated with a first-order decay exponential function versus time (Eq. 3) to obtain *k,* the kinetic coefficient.

$$C = C_0 \cdot \exp(-k \cdot t) \quad (3)$$

The extent of the contaminant conversion was estimated according to Eq. 4.

$$\%\, conversion = 100 \cdot \frac{C_0 - C_t}{C_0} \quad (4)$$

where C_0 and C_t are the contaminant concentrations before the treatment and after treatment of duration t, respectively.

The extent of mineralization was determined through TOC (Total Organic Carbon) analyses, by using a Shimadzu TOC-VCSN analyser. As the solutions to be treated were prepared in tap water, before the analyses samples were acidified to pH 2.5 by adding hydrochloric acid, in order to remove the inorganic carbon from the solution by volatilising CO_2. After acidification, TC (Total Carbon) was measured. This procedure was repeated in triplicate on three samples of tap water, untreated and treated solutions, and the average measures were taken. The percentage of mineralization was calculated using Eq. 5

$$\%\, mineralization = 100 \cdot \frac{TC_0 - TC_{min}}{TC_0} \quad (5)$$

Where TC_0 and TC_{min} are the total carbon content, after acidification of the samples, measured respectively in the untreated sample and after 30 and 60 minutes of treatment.

The process energy yield was assessed by determining the values of the G_{50} and EE/O parameters. G_{50}, defining the amount of PFOA degraded per kWh of energy consumed to achieve 50% conversion, was calculated using Eq. 6 (Malik and Vocs, 2010)

$$G_{50}(mg/kWh) = \frac{1.8 \cdot 10^9 \times C_0(mol/L) \times V(L) \times MM(g/mol)}{P(W) \times t_{1/2}(s)} \quad (6)$$

where V is the treated volume, MM is the molar mass of PFOA, P is the mean power of the reactor and $t_{1/2}$ is the time required for the pollutant to achieve 50% conversion ($t_{1/2} = \ln(2)/k$).

EE/O, defining the electric energy required to degrade PFOA by one order of magnitude in a unit volume (1 m^3) of contaminated water, was calculated using Eq. 7 (Nzeribe et al., 2019)

$$EE/O\ (kWh/m^3) = \frac{P(kW) \times t_{0.9}(min) \times 1000}{V(L) \times 60} \quad (7)$$

where $t_{0.9}$ is the time required to achieve 90% degradation ($t_{0.9} = \ln(2.3)/k$), so the final concentration of the contaminant, C_f, corresponds to 10% of C_0 and the term $log(C_0/C_f)$ in the denominator of the original equation (Nzeribe et al., 2019) was considered equal to 1.

3. Results and discussion

3.1. Degradation kinetics and energy efficiency

Plasma induced surfactant degradation was investigated by means of batch experiments to monitor the surfactant residual concentration after selected treatment times in the RAP reactor operated at constant applied power. Representative results obtained in experiments with PFOA and PFOS, run at initial pollutant concentrations within the wide $1 \cdot 10^{-7}$ - $1 \cdot 10^{-4}$ M range, are shown in Fig.s 3a and 3b, respectively. It is evident at a glance that: 1) these are very fast reactions and 2) the degradation rate increases as the pollutant initial concentration is reduced. Concerning the reaction rates, some

215 are indeed too fast to be adequately monitored by the experimental approach adopted. Nevertheless,
216 the experimental results are unequivocally clear and significant, and can be usefully handled, as
217 done in many previous studies, by interpolation with a first order exponential decay function to
218 obtain the corresponding pseudo-first order kinetic coefficient (k, min^{-1}). The derived k values are
219 reported in Figure 3 and in Table 1. The observed inverse dependence of k on the pollutant initial
220 concentration has numerous precedents in the literature and has been attributed to depletion of
221 plasma reactive species by competing reactions with intermediate products formed from the original
222 pollutant along its route to mineralization (Tampieri et al., 2018 and references therein).
223 Remarkably, in the present study very fast kinetics were observed also in highly concentrated PFAS
224 solutions. Thus, 99% degradation of PFOA was achieved within 30 min of plasma treatment of a
225 $1 \cdot 10^{-4}$ M solution (Fig. 3a). Even more remarkably, at an initial concentration of $1 \cdot 10^{-7}$ M greater
226 than 95% conversion was achieved both for PFOA and PFOS in only 2.5 min. These results
227 demonstrate not only the RAP reactor efficiency but also its robustness in performing well over a
228 wide range of pollutant concentrations. Moreover, considering the inverse dependence of
229 degradation rate on pollutant initial concentration and the low PFAS concentrations (typically in the
230 ppb-ppt range) found in the environment (Podder et al., 2021), it is anticipated that RAP treatment
231 of PFAS contaminated waters would be even faster than reported here. Finally, the last entry in
232 Table 1 shows that the treated volume could be increased from 30 to 100 mL without affecting the
233 process rate, which achieved >99% degradation of an originally 4.14 mg/L PFOA solution in only
234 15 min. As a consequence, the process energy efficiency was greatly improved, G_{50} increasing from
235 to 527 to 2070.4 mg/kWh, as discussed later in the paper.
236 In our experiments PFOS turned out to be somewhat more reactive than PFOA, its degradation rate
237 constant k being at least 20% higher than found for PFOA, both at of $1 \cdot 10^{-5}$ and $1 \cdot 10^{-7}$ M initial
238 concentrations (Fig. 3). Previously Lewis et al, (2020) have also observed a faster degradation of
239 PFOS relative to PFOA; however, Hayashi et al., (2015) found much slower PFOS degradation in
240 comparison to PFOA. The contrasting results for a faster degradation of PFOA or PFOS can be

241 attributed to the different types of plasma discharges used under diverse operating conditions in the
242 studies (Table 1).
243 A comparison of RAP performance with the state-of-art in plasma induced PFOA and PFOS
244 degradation is offered in Table 1, which collects relevant published results obtained with lab-scale
245 prototypes and under similar experimental conditions as used in this study. These systems include
246 plasma generated within gas bubbles inside the liquid (entries 1, 3, 4), streamer or leader discharges
247 in contact with the liquid surface (entries 2, 5, 8, 10), submerged reverse vortex gliding arc
248 plasmatron (entry 6), plasma jet inside the liquid (entry 7) and pulsed corona discharge (entry 9).
249 Like RAP, all these systems were designed to suit and exploit the surface-active properties of
250 PFAS. Performance indicators considered in Table 1 are the kinetic pseudo first-order coefficient
251 (k, min^{-1}), and the energy efficiency parameters G_{50} (mg/kWh) and EE/O (kWh/m^3). Since it is
252 generally observed that the values of all three indicators depend on the pollutant initial (Tampieri et
253 al., 2018), it follows that comparisons are meaningful only among experiments performed at the
254 same or at very similar PFOA or PFOS initial concentrations. Focussing on PFOA, it can be seen
255 that degradation in the RAP reactor was the fastest among the available alternatives. Considering
256 highly concentrated solutions first, our k value of 0.19 min^{-1} at a PFOA concentration of 41.4 mg/L
257 is considerably higher than previously obtained at the same PFOA initial concentration (with k
258 values falling within the 0.02 – 0.06 min^{-1} range, entries 1, 2 and 4) or at similar (30 - 100 mg/L)
259 PFOA initial concentrations (with k values falling within the 0.023 – 0.032 min^{-1} range, entries 3, 6
260 and 8). Similar conclusions are drawn for experiments run at lower initial PFOA concentrations.
261 Considering the 4.14 – 8.3 mg/L initial concentration range, PFOA degradation in the RAP reactor
262 was much faster (k was 0.39 – 0.46 min^{-1}, depending on the volume treated, entry 12, this study)
263 than found in a streamer discharge reactor (k was 0.074 min^{-1}, entry 5) and in an underwater DBD
264 plasma jet reactor (k, estimated, was 0.043 min^{-1}, entry 7).

265 Likewise, kinetics of PFOS degradation in the RAP reactor were much faster than previously
266 achieved with nanopulsed corona discharges (entry 9) and DBD discharge over liquid surface in a
267 falling film reactor (entry 10).
268 Energy efficiency of RAP based treatments was also excellent as shown by G_{50} and EE/O data
269 reported in Table 1. Similarly to the kinetic coefficient k, G_{50} and EE/O also depend on the
270 pollutant initial concentration (C_0), although their dependence is not so straightforward to envision
271 and predict. In the literature as well as in our own experience it is generally found that G_{50} increases
272 with increasing C_0, which is consistent with the presence of C_0 in the numerator of eq. 6 which
273 defines G_{50}. However, the same expression contains in the denominator the parameter $t_{½}$ which
274 often depends on C_0, as seen above and further ahead in the paper, although not in an easily
275 predictable way. In conclusion, comparisons of G_{50} should consider only experiments performed at
276 the same or at very similar PFOA or PFOS initial concentrations. The same holds true for EE/O.
277 While C_0 is not explicitly present in the definition of EE/O (eq. 7), the kinetic parameter $t_{0.9}$, which
278 usually depends on C_0, appears in the numerator.
279 Table 1 shows that the values of G_{50} (2364.6 mg/kWh) and EE/O (13.8 kWh/m^3) obtained with
280 RAP at the highest PFOA concentration tested (41.4 mg/L) are way more favourable than those
281 reported for experiments performed at similar initial PFOA concentrations (within the 41.4 - 100
282 mg/L range) using different plasma arrangements, notably: plasma generated in gas bubbles (entries
283 3 (Takeuchi et al., 2014) and 4 (Hayashi et al., 2015), submerged reverse vortex gliding arc plasma
284 (GAP) discharge (entry 6, (Lewis et al., 2020), and self-pulsing plasma discharge (entry 1, (Saleem
285 et al., 2020a). Comparison with the results of Stratton et al. (Stratton et al., 2017) is particularly
286 interesting since we devised for RAP an electrode configuration which is similar to theirs, with the
287 notable difference, however, that in RAP the ground electrode is not fully submerged in the liquid
288 but placed at the liquid/gas interface. This arrangement makes for an important difference since it
289 generates a more extended plasma-liquid interface, characterized by a denser network of radial
290 plasma discharges in contact with the liquid surface (Fig. 1b) and thus with PFAS molecules which

291 have surfactant properties. The resulting advantages can be appreciated by comparing data obtained
292 at similar PFOA initial concentrations, 4.14 mg/L (this work, entry 12) and 8.3 mg/L (Stratton et
293 al., 2017, entry 5). Our G_{50} of 2070 mg/kWh marks a significant improvement with respect to theirs
294 (486 mg/kWh), a performance upgrade which is reflected also in the process rate and conversion, k
295 in RAP being 0.46 min^{-1} (*vs* 0.074 min^{-1} in Stratton et al.) achieving > 99% degradation in 15 min
296 (vs 90% in 30 min in (Stratton et al., 2017).
297 Similarly, PFOS degradation in the RAP reactor was characterized by better efficiency than
298 reported by or estimated for previous related studies, listed in Table 1, in which different types of
299 plasma discharges were used. Our G_{50} value of 893 mg/kWh obtained with a PFOS initial
300 concentration of 5 mg/L is markedly better than results reported in the literature, despite the fact
301 that higher initial PFOS concentrations (e.g. 10 - 100 mg/L, entries 4, 6, 9, 10 and 11, Table 1) were
302 used in these experiments. Particularly interesting is the comparison with results obtained by
303 Mahyar et al, (2019) in experiments with a PFOS initial concentration of 10 mg/L, similar to the 5
304 mg/L concentration of our experiment, using a nano-pulsed corona discharge reactor and a DBD
305 discharge over liquid falling film reactor. Based on G_{50} (893 mg/kW) and EE/O (4.51 kWh/m^3)
306 indicators, the RAP reactor was at least 4 and 27 times more energy efficient, respectively, than the
307 reactors used by Mahyar et al, (2019).
308 Finally, the last entry in Table 1 highlights another most valuable feature of RAP, i.e. its capability
309 of treating larger volumes, thus improving the energy efficiency, without compromising the process
310 fast kinetics. Treatment of 100 mL aliquots of a 4.14 mg/L PFOA solution achieved >99%
311 degradation in only 15 min, with a remarkable G_{50} and EE/O values of 2070.4 mg/kWh 1.02
312 kWh/m^3.

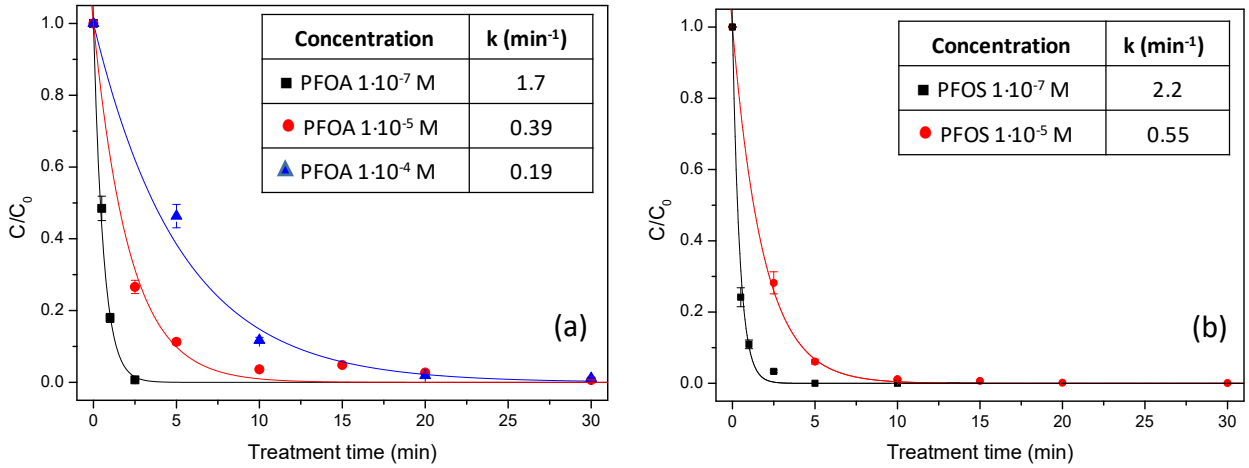

Figure 3. PFAS degradation as a function of time in the RAP reactor operated at 4 W under argon atmosphere. a) PFOA degradation with initial concentrations of $1 \cdot 10^{-4}$ M (41.4 mg/L), $1 \cdot 10^{-5}$ M (4.14 mg/L) and $1 \cdot 10^{-7}$ M (41.4 µg/L). b) PFOS with initial concentrations of $1 \cdot 10^{-5}$ M (5.0 mg/L) and $1 \cdot 10^{-7}$ M (50 µg/L).

As mentioned in the introduction, PFAS are peculiar surfactants with characteristic physical properties and chemical reactivity associated with their high fluorine content. Given the excellent results obtained with PFOA and PFOS, it was of interest to test the scope of RAP applicability in the treatment of surface active pollutants in general. For this purpose the very common non-ionic and fluorine-free surfactant Triton X-100 was also tested in the RAP reactor. Triton X-100 is a polyethylene glycol of $C_{14}H_{22}O(C_2H_4O)_n$ (n = 9-10) composition, terminating with a *p*-(2,4,4-trimethylpentan-3-yl)phenyl ether group (Chart 1). As seen in Fig. 4, RAP performed equally well in treating Triton X-100 as found for PFAS surfactants, the observed k values in experiments run at the same initial concentration of $1 \cdot 10^{-5}$ M being, 0.41, 0.39 and 0.55 min^{-1}, for Triton X-100, PFOA and PFOS, respectively. Interestingly, however, the effect of initial concentration on the degradation rate of Triton X-100 was way less marked than found with PFAS surfactants and only a slight drop in the k value, from 0.41 min^{-1} to 0.38 min^{-1} (i.e. <10%), was observed when a tenfold higher initial concentration ($1 \cdot 10^{-4}$ M) was tested (Fig. 4). This turns out to be a valuable feature, considering that the same energy per unit time was provided in all experiments. An impressive G_{50}

value of 7660 mg/kWh was thus achieved in treating Triton X-100 at an initial concentration of $1 \cdot 10^{-4}$ M, which is ca 10 times higher than that obtained at $1 \cdot 10^{-5}$ M (830 mg/kWh). There is only limited data on the degradation of Triton X-100 using atmospheric plasma in the literature. Aonyas et al, (2016) have reported the efficient degradation of Triton X-100 (at 100 mg/L initial concentration) in a falling film DBD reactor operating at an input power of 180 W. Their estimated G_{50} and EE/O values of 1167 mg/kWh and 75 kWh/m^3, respectively (Aonyas et al., 2016) are however not as efficient as those found in the present study despite the fact that we used a 4-fold lower Triton X-100 initial concentration than theirs. Triton surfactants of different chain length, namely Triton X-45 (n = 4.5) and Triton X-405 (n = 35), were investigated in another study using miniaturized atmospheric pressure glow discharges generated in contact with small sized flowing liquid cathode systems (Jamróz et al., 2014). An estimate of 92-100% degradation was inferred for Triton X-45 30-100 mg/L treated under a 0.6 - 3.2 mL/min flow rate; however, the volume of the solution exposed to plasma and the process energy cost are not specified to make a comparison.

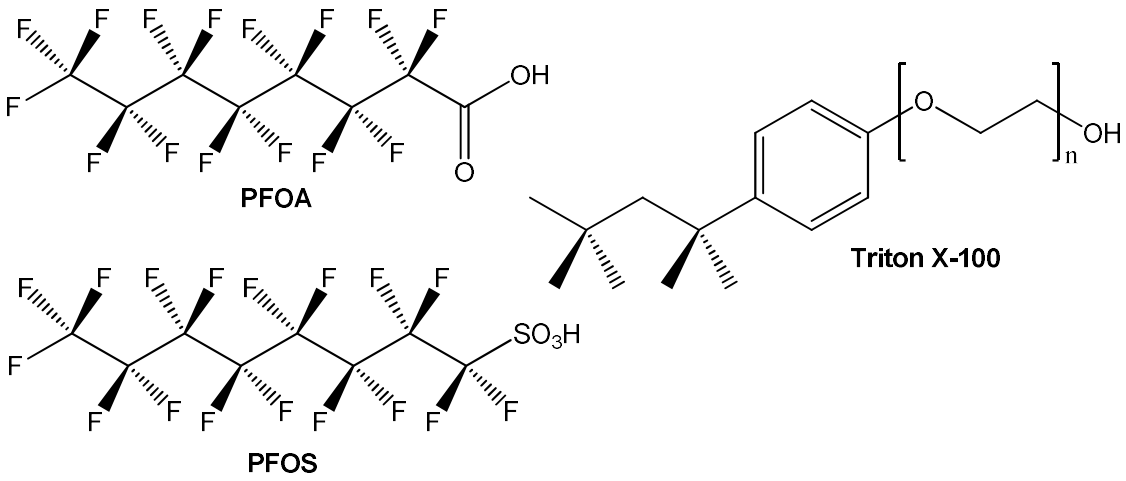

Chart 1

The observed indiscriminate and highly energy-efficient performance of the RAP reactor in comparison to the reported state-of-the-art plasma systems in degrading recalcitrant fluorinated

ionic surfactants (e.g. PFAS) and non-fluorinated non-ionic surfactants (e.g. Triton X-100) demonstrates its high versatility and robustness and motivates efforts for its upgrade and development in applications.

Finally, a comment is due on the different behavior in the kinetics dependence on C_0 observed with Triton X-100 and with PFAS surfactants. With Triton X-100, the C/C_0 profile in time observed in the experiment run with C_0 equal to $1 \cdot 10^{-4}$ M is ca the same as that at $1 \cdot 10^{-5}$ M, indicating that there were sufficient reactive species produced per unit time to attack a tenfold higher number of surfactant molecules. This is clearly not the case for PFAS surfactants suggesting that the difference is due to the ability of Triton X-100 to react directly also with species which are ineffective with PFAS, notably the OH radical.

3.2. PFAS degradation products and mechanisms

Fast and extensive degradation of the original pollutant (≥ 99% within, depending on the PFAS initial concentration, just a few minutes – less than 30 min) is a great result, but likewise important is the chemical composition of the treated water. It is now clearly recognized that the time required for exhaustive degradation of the original pollutant is usually way insufficient to achieve acceptable degrees of mineralization (Ceriani et al., 2018). Product studies are therefore necessary to assess the quality of the treated water. We resorted to TOC analyses, for total dissolved carbon, IC analyses, for released fluoride, and LC-ESI/MS analyses, for identification and quantification of dissolved organic compounds. At high PFOA initial concentration (4.1 mg/L, $1 \cdot 10^{-4}$ M), best suited for optimal analytical response, TOC analysis revealed that a remarkable mineralization extent of 45% and 85% were achieved after a RAP treatment of only 30 and 60 min, respectively, while less than 30 min were sufficient to make any residual PFOA undetectable by LC-ESI/MS analysis, corresponding to concentrations lower than $1.2 \cdot 10^{-9}$ M. Analysis of the solution at various treatment times revealed, in agreement with earlier reports (Saleem et al., 2020a; Singh et al., 2019a;

376 Takeuchi et al., 2014), the presence of small amounts of perfluorinated acid homologues of PFOA
377 with shortened alkyl chain, notably $C_nF_{2n+1}COOH$ with n = 6, 5, 4. Additional very minor products
378 were also observed, specifically polyfluorinated acids in which one or two fluorine atoms are
379 replaced by hydrogen atoms (Singh et al., 2019a). The time profiles of the concentration of PFOA
380 and of its $C_nF_{2n+1}COOH$ products are shown in Figure 5a. It is seen that as the concentration of
381 PFOA decreases, those of its degradation products perfluoroheptanoic acid (PFHpA) and
382 perfluorohexanoic acid (PFHxA) increase in time, reach a maximum and then decay, as is typical of
383 reaction intermediates which form and in turn react in the system. In the case of perfluoropentanoic
384 acid (PFPA), the concentration is still increasing after 30 min treatment, supporting the
385 interpretation found in the literature (Singh et al., 2019a) that PFOA degradation to give lower
386 homologues occurs orderly via sequential chain shortening steps and not via random C-C bond
387 breaking along the chain. The sum of all detected degradation products after a plasma treatment of
388 30 min amounted to only 6% of the total organic carbon initially present as PFOA, suggesting that
389 organic products are formed which are undetected by these analyses. At lower PFOA initial
390 concentration (41.4 μg/L, $1 \cdot 10^{-7}$ M) the degradation is much faster and no peaks due either to PFOA
391 or to any organic product could be detected by LC-ESI/MS after a treatment time of only 2.5 min.
392 Interestingly, the same $C_nF_{2n+1}COOH$ products, including in this case also PFOA (n = 7), were also
393 detected in the reaction of PFOS (initial concentration: 5 mg/L, $1 \cdot 10^{-5}$ M) although their time
394 evolution is not as clear to interpret (Figure 5b).
395 Scheme 1 summarizes the mechanism proposed for PFOA degradation to form $C_nF_{2n+1}COOH$
396 homologues with shortened alkyl chain and that for PFOS conversion into PFOA. All steps and
397 short-lived reaction intermediates have precedents in the literature (Cui et al., 2020; Niu et al.,
398 2012; Singh et al., 2019b).

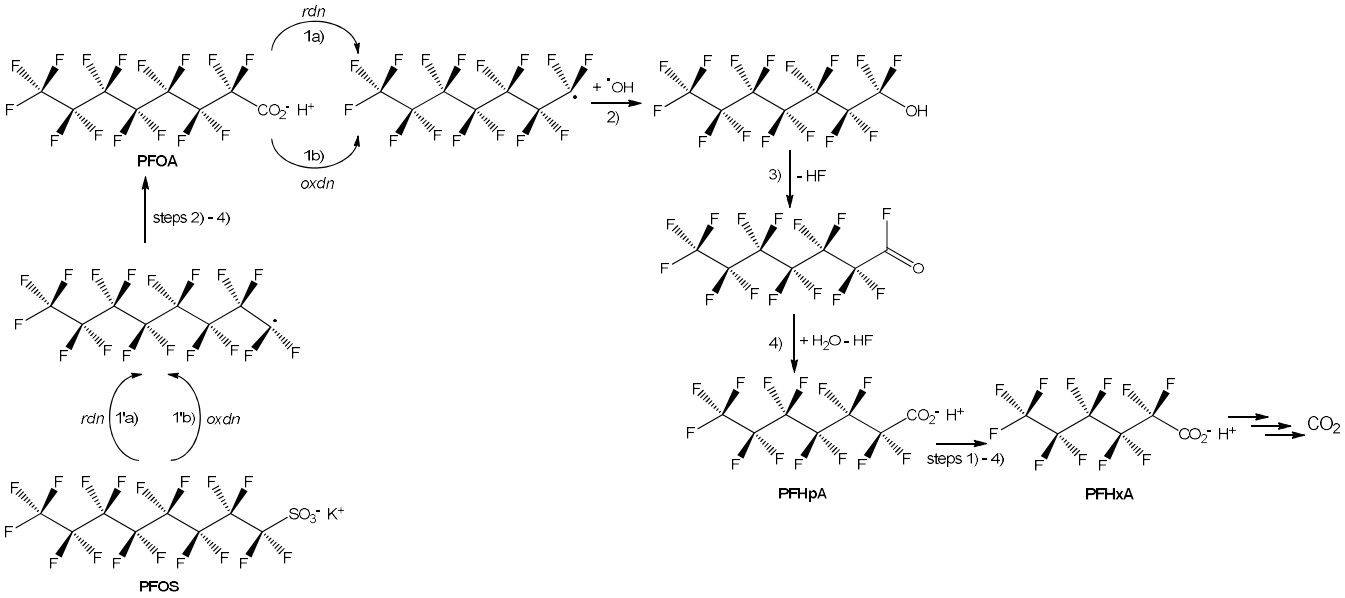

399
400

401 **Scheme 1.** Proposed mechanism for identified PFOA and PFOS degradation pathways

402

403 The scheme shows that PFOA degradation may be initiated either by a reductant (1a) or by an
404 oxidant (1b), leading in any case to the same reactive intermediate, the perfluoroalkyl radical $\cdot C_7F_{15}$.
405 In path 1a free or hydrated electrons are involved to form via electron attachment a very reactive
406 perfluorooctanoate radical ion, $[C_7F_{15}CO_2^-]^{\cdot-}$. Protonation of this very strong base and elimination of
407 carbon monoxide (CO) and hydroxide (HO^-) gives the perfluoroalkyl radical $\cdot C_7F_{15}$. Alternatively,
408 perfluorooctanoate can undergo one electron oxidation (1b) to the corresponding radical,
409 $C_7F_{15}CO_2\cdot$, which eliminates CO_2 to form the same intermediate $\cdot C_7F_{15}$ seen above. It has been
410 proposed previously (Singh et al., 2019a) that Ar^+ formed by discharges in argon is a strong enough
411 oxidant to bring about one electron oxidation of perfluorooctanoate. Regardless of its genesis, i.e.
412 via perfluorooctanoate reduction (1a) or oxidation (1b), the perfluoroheptyl radical reacts with an
413 OH radical to form perfluoroheptanol (step 2) which is unstable and undergoes HF elimination to
414 the corresponding acyl fluoride (step 3). This intermediate is also highly reactive and in water
415 undergoes hydrolysis to perfluoroheptanoate (step 4), the PFOA homologue with one less carbon in
416 the alkyl chain. The sequence of steps 1) – 4) reiterates until complete mineralization is achieved in

a sequential orderly way as shown in Scheme 1. It should be noted that OH radicals, which are known to be unable to attack perfluorocarboxylates, are nevertheless involved in a crucial step of their degradation (step 2). Scheme 1 also accounts for the observed production of perfluorooctanoate and lower homologues in the plasma activated degradation of PFOS. Similarly to PFOA, two possible initiation steps are proposed for PFOS degradation, reduction (step 1'a) and oxidation (step 1'b), both leading to the same perfluorooctyl radical reactive intermediate (Singh et al., 2019a). One electron reduction of perfluoroalkyl sulfonates which dissociates via C-S bond cleavage has been proposed previously for reactions with hydrated electrons (Bentel et al., 2019). Similarly one electron oxidation of perfluoroalkyl sulfonates is a well known process, occurring in electrochemical oxidation processes (Niu et al., 2016) and forming the perfluorooctylsulfonyl radical which dissociates to sulfur trioxide (SO_3) and perfluorooctyl radical. In argon plasma activated process one electron oxidation of PFOS might occur via electron transfer to Ar^+, as proposed for PFOA (Singh et al., 2019a).

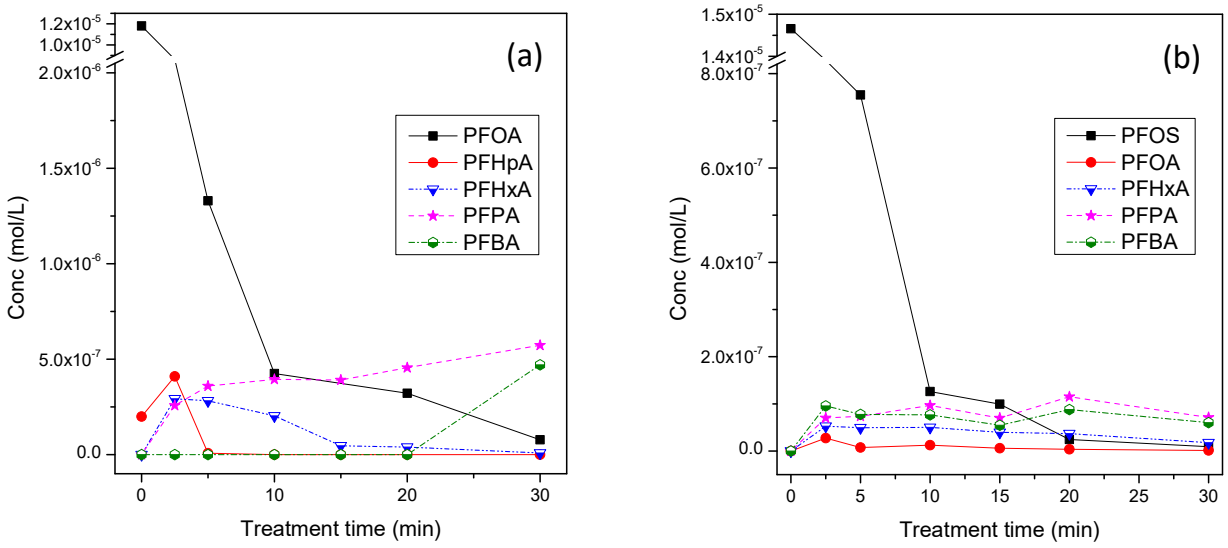

Figure 5. Time profiles of the concentration of PFOA (a) and PFOS (b) and of their degradation products during treatment of $1 \cdot 10^{-5}$ M solutions in tap water in the RAP reactor operated at 4 W under argon atmosphere.

435 Finally, it should be mentioned that trace amounts of perfluoroheptane and perfluorohexane
436 sulfonates were also detected by our analyses in experiments run with PFOS (data not shown). We
437 note that perfluorohexane and perfluorobutane sulfonates were detected in a previous investigation
438 of PFOS degradation activated by an argon plasma (Singh et al., 2019a), and proposed to be
439 reaction products formed by trapping of the corresponding perfluoroalkyl radicals, $\cdot C_6F_{13}$ and $\cdot C_4F_9$,
440 respectively, by $SO_3^{-\bullet}$. We found no evidence for such a sulfonate chain shortening process in our
441 system, while the detected lower homologues of PFOS, i.e. perfluoroheptane and perfluorohexane
442 sulfonates, were already present at time zero as impurities in the commercial PFOS sample used.
443 Expectedly, both impurities were degraded in time, according to the mechanism described in
444 Scheme 1.

Table 1. Comparison of different types of atmospheric plasma for PFOA degradation

S. No	Plasma type / reactor configuration	Plasma gas	Power supply	Treated volume (mL)	PFAS initial concentration		Plasma input power (W)	% degradation	k (min^{-1})	% defluorination	G_{50} (mg/kWh)	EE/O (kWh/m^3)	References
1	Bubbling from HV hollow electrode, DBD quartz reactor, without cooling	Synthetic air (80% N_2 and 20% O_2)	AC, 50 Hz, 12 kV, 30 mA, DBD reactor	15	PFOA	41.4 mg/L	7	49% in 30 min	0.02	-	78	*3034	(Saleem et al., 2020a)
2	Self-Pulsing discharge over liquid surface, grounded liquid electrode, without cooling	Argon	DC, 30kV, 12 mA, 3nF	15	PFOA	41.4 mg/L	2.89	89% in 30 min	0.06	47% in 30 min	561	*128	(Saleem et al., 2020a)
3	Bubbling from a single hole, grounded liquid electrode, with cooling	Oxygen	DC, 30 kV, 40 mA	20	PFOA	64.6 mg/L	10	97.4% in 150 min	*0.032	-	*136	*500	(Takeuchi et al., 2014)
4	Bubbling from a single hole, grounded liquid electrode, with cooling	Oxygen	DC, 30 kV, 40 mA	20	PFOA	41.4 mg/L	32	98% in 180 min	*0.033	94.5% in 180 min	*39	*1042	(Hayashi et al., 2015)
					PFOS	60 mg/L	32	100% in 480 min			*42	*341	
5	Streamer/leader discharge over Liquid surface with liquid recirculation, grounded liquid electrode, without cooling	Argon	Pulsed DC, 120 Hz, 25 kV (high rate) 20 Hz, 16 kV (high efficiency)	1400	PFOA	8.3 mg/L	76.5 (high rate), 4.1 (high efficiency)	90% (high rate) and 25% (high efficiency) in 30 min	0.074 (high rate), 0.012 (high efficiency)	*27% (high rate) and *4.6% (high efficiency) in 30 min	*486.5 (high rate), 1472 (high efficiency)	*28 (high rate), *75 (high efficiency)	(Stratton et al., 2017)
6	Submerged non-equilibrium, reverse vortex gliding arc plasma with liquid recirculation, without cooling	Compressed humid air		1000	PFOA	100 mg/L	150	21% in 20 min	-	17% in 20 min	-	213.4	(Lewis et al., 2020)
					PFOS	100 mg/L	180	25% in 1 min	-	-	-	23.2	

7	Under water DBD-plasma jet	Air	AC (1-5 kHz) and nano-second pulsed DC 1-10 kHz)	500	PFOA	5.7 mg/L	25	92.3% in 60 min	*0.043	-	-	45	(Groele et al., 2021)
8	Needles-plate pulsed discharge over liquid surface with micro bubbling.	Argon and Air	Pulsed power supply 1-60 kV	300	PFOA	30 mg/L	38.9	95.3 % (Ar), 81.5 % (Air) in 2 h	0.023 (Ar), 0.015 (Air)	50.7 % (Ar), 44.8 % (Air) in 2 h	230.3 (Ar), 150.2 (Air)	216.5 (Ar), 332 (Air)	(Zhang et al., 2021)
9	Nano-pulsed corona, grounded liquid electrode, without cooling	Helium and Argon	DC Nano-pulse, 20 ns pulses, 15-18 kV, 2 kHz	7500	PFOS	10 mg/L	110 (He), 130 (Ar)	83% (He), 88% (Ar) in 360 min	0.005 (He), 0.006 (Ar)	25% (He), 43% (Ar) in 360 min	170 (He), 220 (Ar)	*148 (He), *123 (Ar)	(Mahyar et al., 2019)
10	DBD discharge over liquid surface in planar falling film reactor, grounded liquid electrode, without cooling	Helium and Argon	AC generator, 21 kV 200 W; 5-20 kHz in burst mode	400	PFOS	10 mg/L	200	97% (He), 98% (Ar) in 45 min	0.11 (He), 0.09 (Ar)	14% (He), 25% (Ar) in 30 min	71 (He), 35 (Ar)	*162 (He), *130 (Ar)	(Mahyar et al., 2019)
11	Nanosecond pulsed discharge plasma generated with fine droplets	Oxygen	Nanosecond pulsed discharge generator, 40 kV, 400 Hz	1000	PFOS	50 mg/L	32	*58% in 180 min	0.0054	*22% in 180 min	*365	*82	(Takeuchi et al. 2020)
12	Radial plasma discharge over liquid surface, bubbling from the bottom, without cooling	Argon	DC –, 30kV, 12 mA, 2.1nF, 60-80 Hz	30	PFOS	5.0 mg/L, ($1\cdot10^{-5}$ M)	4	>99% in 10 min	0.55	-	893.1	4.51	This study
						50 µg/L, ($1\cdot10^{-7}$ M)	4	96.7% in 2.5 min	2.2	-	35.2	1.6	
				30	PFOA	41.4 mg/L, ($1\cdot10^{-4}$ M)		98.9% in 30 min	0.19	64.4% in 30 min	2364.6	13.8	
						4.14 mg/L, ($1\cdot10^{-5}$ M)	4	99.3% in 30 min	0.39	58.5% in 30 min	527	6.0	
						41.4 µg/L, ($1\cdot10^{-7}$ M)		>99% in 2.5 min	1.7	-	22.5	3.9	
				100		4.14 mg/L, ($1\cdot10^{-5}$ M)	4	>99% in 15 min	0.46	-	2070.4	1.02	

*Calculated from data or estimated from figures reported in the article.

Conclusions

Strengths and limitations of available physical-chemical techniques for PFAS destruction, including electrochemical oxidation, advanced reduction processes, plasma-based technology, sonolysis, heat-activated persulfate and photochemical oxidation, were recently reviewed (Nzeribe et al., 2019). In comparative assessments, plasma based technology placed among the best performing in terms of the process effectiveness (extent of mineralization) and efficiency (kinetics and energy costs) (Nzeribe et al., 2019). The described new radial plasma discharge reactor (RAP) performed remarkably well in treating water contaminated by common PFAS surfactants perfluorooctanoate (PFOA) and perfluorooctyl sulfonate (PFOS) with respect to most significant process indicators: degradation kinetics, conversion extent, amount of byproducts and energy consumption. Remarkably, > 99% PFOA conversion was achieved in 2.5 min treatment of a 41.4 μg/L solution, with side products being below our analytical PFAS detection threshold. Trade-off between short treatment times and high energy costs is an issue to be properly exploited depending on PFAS concentrations found in specific applications. Indeed energy efficiencies as high as 2365 mg/kWh were achieved in the treatment of concentrated PFOA solutions (41.4 mg/L), which however required longer treatment times (99% conversion in 30 min). The volume of treated solution is another important issue. Most remarkably, with RAP the volume could be increased from 30 to 100 mL without compromising the process rate but greatly gaining in energy efficiency, G_{50} increasing from 527 to 2070.4 mg/kWh. The excellent performance of RAP in degrading PFAS surfactants is attributed to the very extended area of contact between discharge and liquid surface achieved in this setup. Excellent results were also obtained with the non-ionic fluorine free surfactant Triton X-100, indicating that the scope of RAP application covers surfactants in general and demonstrating the potential of this approach as a versatile and robust stage of advanced reduction/oxidation processes (ARP/AOP) in water treatment trains.

Acknowledgments

Financial funds supporting Mubbshir Saleem and the research activities are gratefully acknowledged (University of Padova, P-DiSC#06BIRD2019-UNIPD). LC-ESI/MS analyses were performed with a Thermo Scientific LTQ XL mass spectrometer funded by the "Dipartimenti di Eccellenza" Grant "NExuS", awarded to the Department of Chemical Sciences of University of Padova by the Italian Ministry for Education, University and Research (MIUR). The authors acknowledge the technical support from Mauro Meneghetti and Stefano Mercanzin for the construction of the plasma reactor.

References

Aonyas, M.M., Nešić, J., Jović, M., Marković, M., Dojčinović, B., Obradović, B., Roglić, G.M., 2016. Degradation of Triton X-100 in Water Falling Film Dielectric Barrier Discharge Reactor. Clean - Soil, Air, Water 44, 422–429. doi:10.1002/clen.201500501

Bentel, M.J., Yu, Y., Xu, L., Li, Z., Wong, B.M., Men, Y., Liu, J., 2019. Defluorination of Per- and Polyfluoroalkyl Substances (PFASs) with Hydrated Electrons: Structural Dependence and Implications to PFAS Remediation and Management. Environmental Science and Technology 53, 3718–3728. doi:10.1021/acs.est.8b06648

Bulusu, R.K.M., Wandell, R.J., Zhang, Z., Farahani, M., Tang, Y., Locke, B.R., 2020. Degradation of PFOA with a nanosecond-pulsed plasma gas–liquid flowing film reactor. Plasma Processes and Polymers 17, 1–6. doi:10.1002/ppap.202000074

Ceriani, E., Marotta, E., Shapoval, V., Favaro, G., Paradisi, C., 2018. Complete mineralization of organic pollutants in water by treatment with air non-thermal plasma. Chemical Engineering Journal 337, 567–575. doi:10.1016/j.cej.2017.12.107

Cui, J., Gao, P., Deng, Y., 2020. Destruction of Per- and Polyfluoroalkyl Substances (PFAS) with Advanced Reduction Processes (ARPs): A Critical Review. Environmental Science &

Technology. doi:10.1021/acs.est.9b05565

Groele, J.R., Sculley, N., Olson, T.M., Foster, J.E., 2021. An investigation of plasma-driven decomposition of per- and polyfluoroalkyl substances (PFAS) in raw contaminated ground water. Journal of Applied Physics 130, 053304. doi:10.1063/5.0039264

Hayashi, R., Obo, H., Takeuchi, N., Yasuoka, K., 2015. Decomposition of Perfluorinated Compounds in Water by DC Plasma within Oxygen Bubbles. Electrical Engineering in Japan (English translation of Denki Gakkai Ronbunshi) 190, 9–16. doi:10.1002/eej.22499

Jamróz, P., Gręda, K., Pohl, P., Żyrnicki, W., 2014. Atmospheric pressure glow discharges generated in contact with flowing liquid cathode: Production of active species and application in wastewater purification processes. Plasma Chemistry and Plasma Processing 34, 25–37. doi:10.1007/s11090-013-9503-3

Kah, M., Oliver, D., Kookana, R., 2021. Sequestration and potential release of PFAS from spent engineered sorbents. Science of the Total Environment 765, 142770. doi:10.1016/j.scitotenv.2020.142770

Lewis, A.J., Joyce, T., Hadaya, M., Ebrahimi, F., Dragiev, I., Giardetti, N., Yang, J., Fridman, G., Rabinovich, A., Fridman, A.A., McKenzie, E.R., Sales, C.M., 2020. Rapid degradation of PFAS in aqueous solutions by reverse vortex flow gliding arc plasma. Environmental Science: Water Research and Technology 6, 1044–1057. doi:10.1039/c9ew01050e

Mahyar, A., Miessner, H., Mueller, S., Hikmat, K., Aziz, H., Kalass, D., Moeller, D., Kretschmer, K., Robles, S., 2019. Development and application of different non‐thermal plasma reactors for the removal of perfluorosurfactants in water: A comparative study. Plasma Chemistry and Plasma Processing 39, 531–544. doi:10.1007/s11090-019-09977-6

Malik, M.A., Vocs, D.Á., 2010. Water Purification by Plasmas : Which Reactors are Most Energy Efficient ? Plasma Chemistry and Plasma Processing Plasma Che, 21–31. doi:10.1007/s11090-009-9202-2

Marotta, E., Ceriani, E., Schiorlin, M., Ceretta, C., Paradisi, C., 2012. Comparison of the rates of

phenol advanced oxidation in deionized and tap water within a dielectric barrier discharge reactor. Water Research 46, 6239–6246. doi:10.1016/j.watres.2012.08.022

Niu, J., Li, Y., Shang, E., Xu, Z., Liu, J., 2016. Electrochemical oxidation of perfluorinated compounds in water. Chemosphere 146, 526–538. doi:10.1016/j.chemosphere.2015.11.115

Niu, J., Lin, H., Xu, J., Wu, H., Li, Y., 2012. Electrochemical mineralization of perfluorocarboxylic acids (PFCAs) by Ce-doped modified porous nanocrystalline PbO2 film electrode. Environmental Science and Technology 46, 10191–10198. doi:10.1021/es302148z

Nzeribe, B.N., Crimi, M., Mededovic Thagard, S., Holsen, T.M., 2019. Physico-Chemical Processes for the Treatment of Per- And Polyfluoroalkyl Substances (PFAS): A review. Critical Reviews in Environmental Science and Technology 49, 866–915. doi:10.1080/10643389.2018.1542916

Obo, H., Takeuchi, N., Yasuoka, K., 2015. Decomposition of perfluorooctanesulfonate (PFOS) by multiple alternating argon plasmas in bubbles with gas circulation. International Journal of Plasma Environmental Science and Technology 9, 62–68.

Podder, A., Sadmani, A.H.M.A., Reinhart, D., Chang, N. Bin, Goel, R., 2021. Per and poly-fluoroalkyl substances (PFAS) as a contaminant of emerging concern in surface water: A transboundary review of their occurrences and toxicity effects. Journal of Hazardous Materials 419, 126361. doi:10.1016/j.jhazmat.2021.126361

Rabinovich, A., Nirenberg, G., Kocagoz, S., Surace, M., Sales, C., Fridman, A., 2022. Scaling Up of Non-Thermal Gliding Arc Plasma Systems for Industrial Applications. Plasma Chemistry and Plasma Processing 42, 35–50. doi:10.1007/s11090-021-10203-5

Saleem, M., Biondo, O., Sretenović, G., Tomei, G., Magarotto, M., Pavarin, D., Marotta, E., Paradisi, C., 2020a. Comparative performance assessment of plasma reactors for the treatment of PFOA; reactor design, kinetics, mineralization and energy yield. Chemical Engineering Journal 382, 123031. doi:10.1016/j.cej.2019.123031

Saleem, M., Marotta, E., Paradisi, C., 2020b. Radial-Discharge Plasma Reactor, for treatment of

548 contaminant liquids, Italian patent application nr.102020000021772, 2020/09/15; PCT
549 international application nr. PCT/IB2021/057137, 2021/08/04) 1–14.
550 Singh, R.K., Fernando, S., Baygi, S.F., Multari, N., Thagard, S.M., Holsen, T.M., 2019a.
551 Breakdown Products from Perfluorinated Alkyl Substances (PFAS) Degradation in a Plasma-
552 Based Water Treatment Process. Environmental Science and Technology 53, 2731–2738.
553 doi:10.1021/acs.est.8b07031
554 Singh, R.K., Multari, N., Nau-Hix, C., Anderson, R.H., Richardson, S.D., Holsen, T.M., Mededovic
555 Thagard, S., 2019b. Rapid Removal of Poly- and Perfluorinated Compounds from
556 Investigation-Derived Waste (IDW) in a Pilot-Scale Plasma Reactor. Environmental Science
557 and Technology 53, 11375−11382. doi:10.1021/acs.est.9b02964
558 Stratton, G.R., Dai, F., Bellona, C.L., Holsen, T.M., Dickenson, E.R.V., Mededovic Thagard, S.,
559 2017. Plasma-Based Water Treatment: Efficient Transformation of Perfluoroalkyl Substances
560 in Prepared Solutions and Contaminated Groundwater. Environmental Science and
561 Technology 51, 1643–1648. doi:10.1021/acs.est.6b04215
562 Takeuchi, N., Kitagawa, Y., Kosugi, A., Tachibana, K., Obo, H., Yasuoka, K., 2014. Plasma-liquid
563 interfacial reaction in decomposition of perfluoro surfactants. Journal of Physics D: Applied
564 Physics 47. doi:10.1088/0022-3727/47/4/045203
565 Takeuchi, N., Suzuki, D., Okada, K., Kazuki, O., Kodama, S., Namihira, T., Wang, D., 2020.
566 Discharge conditions for efficient and rapid decomposition of perfluorooctane sulfonic acid
567 (PFOS) in water using plasma. International Journal of Plasma Environmental Science and
568 Technology 14, 12pp.
569 Tampieri, F., Giardina, A., Bosi, F.J., Pavanello, A., Marotta, E., Zaniol, B., Neretti, G., Paradisi,
570 C., 2018. Removal of persistent organic pollutants from water using a newly developed
571 atmospheric plasma reactor. Plasma Processes and Polymers 15. doi:10.1002/ppap.201700207
572 Thagard, S.M., Locke, B.R., 2022. Special Issue of Plasma Chemistry and Plasma Processing
573 Scale-Up of Plasma Reactors for Bio, Chemical, Environmental, Materials, and Energy

574 Applications. Plasma Chemistry and Plasma Processing 42, 1–2. doi:10.1007/s11090-021-
575 10227-x
576 Trojanowicz, M., Bojanowska-czajka, A., Bartosiewicz, I., Kulisa, K., 2018. Advanced Oxidation /
577 Reduction Processes treatment for aqueous perfluorooctanoate (PFOA) and
578 perfluorooctanesulfonate (PFOS) – A review of recent advances. Chemical Engineering
579 Journal 336, 170–199. doi:10.1016/j.cej.2017.10.153
580 Zhang, H., Li, P., Zhang, A., Sun, Z., Liu, J., Héroux, P., Liu, Y., 2021. Enhancing Interface
581 Reactions by Introducing Microbubbles into a Plasma Treatment Process for Efficient
582 Decomposition of PFOA. Environmental Science and Technology 55, 16067–16077.
583 doi:10.1021/acs.est.1c01724
584